Electrochemical Noise Generation during SCC of a High-Strength Carbon Steel ☆

R.A. Cottis* and C.A. Loto**

ABSTRACT

Stress-corrosion cracking experiments have been performed on a high-strength carbon steel exposed to acidified sodium chloride solution poisoned with sodium sulfide. The electrochemical potential of the specimen was monitored during the experiment, and this paper reports the observed electrochemical noise. The analysis was performed using both the maximum entropy method and the discrete Fourier transform. A consistent noise behavior was observed throughout the experiment, with the only perturbation of any significance being associated with major transients that occurred when the specimen actually failed. The average noise power measured over a period of the same order as the duration of the transients has been found to be an effective method of detecting them, but it is expected that this will be much more difficult in service conditions.

KEY WORDS: electrochemical, frequency, noise generation, power spectra, stress corrosion, time record.

INTRODUCTION

Noise is a general term used to describe the fluctuating behavior of a physical variable with time. For an electrochemical process one may measure either the voltage noise (i.e., the fluctuation in the electrochemical potential with time) or the current noise (e.g., the fluctuation of galvanic current flowing between two specimens or the fluctuation in applied current in a potentiostatic experiment). For this work the voltage noise has been studied, and this introduction will concentrate on this mode of measurement, although it will be appreciated that current noise measurements are similar in most respects.

The phenomenon of electrochemical noise and the information that it may provide on corrosion processes has received considerable attention in recent years.[1-5] The analysis of electrochemical noise is now considered to give useful information about the rate and nature of electrochemical processes taking place at the electrode, although the theoretical basis of much of the interpretation is somewhat limited. For a pure activation-controlled process the source of the noise is thought to be the stochastic fluctuation of the rates of the forward and reverse reactions. In the more common case (for corrosion) of reaction at filmed interfaces the source of the noise is somewhat less clear, but it tends to be attributed to the breakdown and repair of the film. Other processes

---

☆ Submitted for publication October 1986; revised August 1988.

* Corrosion and Protection Centre, UMIST, P. O. Box 88, Manchester M60 1QD, UK.

** Department of Mechanical Engineering, University of Lagos, Akoka, Yaba, Lagos, Nigeria.

0010-9312/90/000003/$3.00/0

that can be expected to give rise to noise are the unstable initiation and repassivation of pits, crevice corrosion, fluctuations in convective mass-transport, and the growth of a stress-corrosion crack. As the several mechanisms proposed for the growth of stress-corrosion cracks may be expected to have different electrochemical noise characteristics, it was felt to be useful to determine these characteristics for systems with reasonably well-understood mechanisms of crack growth.

In this work the electrochemical noise generated during the SCC of a high-strength carbon steel freely corroding in a deaerated, acidified NaCl solution has been studied, and the noise emitted correlated with the progress of the stress corrosion test. SCC in this metal-environment system is almost certainly due to hydrogen embrittlement, and it was expected that the cracking would occur by a discontinuous, essentially mechanical process, with the main source of noise being associated with the intermittent exposure of fresh surface to the solution.

EXPERIMENTAL PROCEDURE

Material

The material used for these tests was purchased as "gauge plate," mainly because this provided a good-quality high-carbon steel in the form of thin surface-ground sheet. The composition of the material was: 0.95C, 0.35Si, 1.27Mn, 0.019S, 0.018P, 0.16Ni, 0.06Cr, 0.08Mo, 0.12V, 0.02Co, 0.002Ti, 0.028Nb, 0.23Cu, 0.05A1, 0.04Sn and 0.017Pb. This was cut into blanks 120 mm long, 10 mm wide, and 1 mm thick. Preparation of the specimen involved heat treatment followed by polishing. Heat treatment consisted of austenitization in argon at 800°C for 2 hours, followed by oil quenching. The specimens were then tempered at 207°C for 1 hour. This heat treatment gave an ultimate tensile strength (UTS) of 2274 MPa and a Brinell Hardness of 680. The surfaces of the specimens were prepared by polishing with abrasive paper down to 1200 grit, followed by 3 and 1 μm diamond.

Sample Loading

The specimens were loaded in buckling using a simple bolt-loaded clamp which is shown in Figure 1. The main feature of this loading is the loading washer, which contains an annular groove into which the end of the specimen fits, thereby ensuring reasonably precise alignment. A large-diameter (20-mm) bolt was used to maximize the stiffness of the loading jig. The stress in the specimen was determined by measuring its curvature with a dial gauge mounted on a U-section stand, the stress in the outer fibers being calculated from the relationship:

$$S = \frac{4Etd}{l^2}$$

where

S = Stress in outer fiber
E = Young's modulus
d = Distance of center of arc to the chord
t = Specimen thickness
l = Length of chord

Environment

The solution used was 3.5% sodium chloride solution, to which 500 ppm of sodium sulfide was added as a hydrogen recombination poison. Shortly before the experiment, the solution was acidified with H_2SO_4 to a pH of 2. Additionally, the solution was deaerated with nitrogen in order to reduce the competitive effect of oxygen on the cathodic reaction. As a result of the low pH the sulfide would have been present predominantly in the form of H_2S, some of which will have been removed by the deaeration, but this still results in an environment with a very strong tendency to generate hydrogen, which dissolves in the steel.

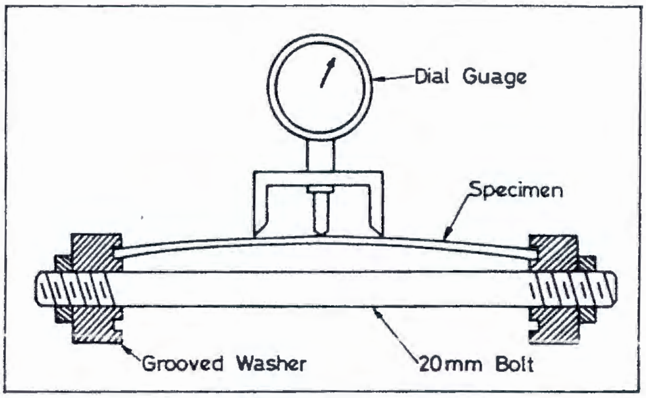

FIGURE 1. *Specimen configuration and loading jig.*

Time-to-Failure Tests

In order to provide a baseline for the electrochemical noise measurements the time-to-failure was determined for specimens stressed to a range of values. The time to-failure was monitored visually, and by means of a record of the specimen potential. The results are shown in Figure 2. As might be expected for a very high-strength steel in an aggressive environment, failure occurs rapidly, even at relatively low stresses.

Electrochemical Noise Measurement

For studies of electrochemical noise, the specimens were stressed to 796 MPa (35% of the yield stress), giving a time-to-failure of approximately $2\frac{1}{2}$ hours. The loading jig was supported above the surface of the solution, so that only the stressed steel was exposed to the solution. The electrochemical potential of the specimen was measured with respect to a saturated calomel reference electrode. The measurement was made with a Solartron(1) 7055 digital voltmeter. This was controlled by a Hewlett Packard(2) HP85 desk-top computer, which also served to record the readings on magnetic tape. Time records consisted of blocks of 1024 readings taken at one second intervals. Allowing for a delay of about 3 minutes while the readings were written to tape at the end of the time record, each reading took approximately 20 minutes. Other than the delay in storing the data onto the tape, time records were taken continuously, hence about eight time records were taken over the duration of a typical test.

Data Analysis

It is not clear that an optimum method has yet been developed for the presentation and interpretation of electrochemical noise data. The most common approach used is to transform the data from the time domain (i.e., the time record) to the frequency domain to give a spectrum of the power density present at any given frequency. This is a common technique in various fields of physical science, particularly communications engineering, and several algorithms have been developed to perform this tranformation. Unfortunately, none of these are without difficulties when applied to typical corrosion time records, since they must all make assumptions about the properties of the variable being studied. In general the mathematically rigorous techniques assume that the variable is stationary, i.e., all its statistical properties such as mean and variance do not change with time. This tends to be a questionable assumption for corrosion processes; in particular the mean value of electrochemical potential is frequently observed to drift with time. The variance may well change with time as well, although this is more difficult to detect by inspection of the time record.

---

(1) Solartron Instrumentation Group, Sangamo Weston, Inc., Irvine, CA.
(2) Hewlett Packard Co., Precision Instruments, Palo Alto, CA.

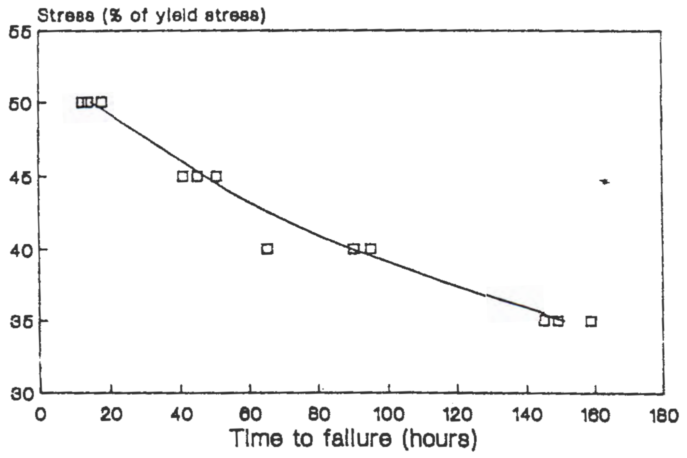

FIGURE 2. *Time-to-failure as a function of applied stress.*

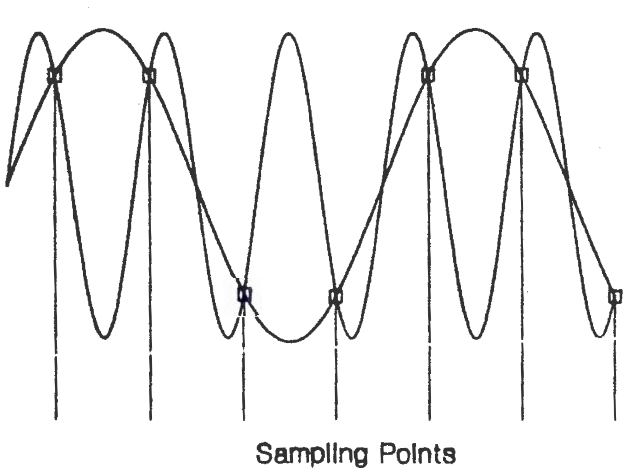

FIGURE 3. *Sampling of a continuous waveform and aliasing of high-frequency components.*

In order to convert a signal that is subject to drift into a better approximation of a stationary process, it is common practice to perform a trend-removal process before analysis. In its simplest form this entails the fitting of a straight line to the original data, and then using the deviation of individual points from the straight line as the new data set. In more extreme cases a higher order polynomial may be used in place of a straight line, but it should be appreciated that all of these techniques are eliminating low frequency information in the data, with the higher order polynomials having a more severe effect.

The process of sampling the data also introduces difficulties where high frequency signals are concerned. For frequencies of less than half the sampling frequency one may expect to obtain a reasonable reconstruction of the original waveform (see Figure 3), and a reasonably accurate measurement of the power spectral density. For the special case of a signal of exactly half the sampling frequency (known as the Nyquist frequency), essentially any value of power spectral density between zero and the true value may be obtained, deriding on the phase relationship between the signal and the sampling window. For signal frequencies above the Nyquist frequency, the phenomenon of *aliasing* transforms the high-frequency signal to a fictitious signal of the same amplitude, but at a lower frequency. Potentially this is a serious problem, and anti-aliasing filters should be used to remove these frequencies from the signal before it is sampled, since it is impossible to do anything after sampling (note in Figure 3 that the sampled data from the genuine low-frequency signal, and those produced by aliasing of the high-frequency signal are identical). In practice electrochemical noise tends to have less power at the higher frequencies, and aliasing is not a major practical problem, although it may cause some distortion of the higher frequency end of the power spectrum (this is discussed further below).

For this work two data analysis techniques have been used. The discrete Fourier transform in the form of the fast Fourier transform (FFT) is the most common method of transforming data from the time domain to the frequency domain, although it does have certain difficulties. An alternative solution that has received some attention for the analysis of electrochemical noise is the maximum entropy method (MEM), developed by Burg.[6]

In addition to removing trends as described above, for the discrete Fourier transform it is also necessary to 'blend' the signal to zero at each end of the time record in order to eliminate false components in the spectrum (this is because an inherent assumption of the Fourier transform is that the time record is repeated indefinitely). This is achieved by the use of a windowing function, which may take various forms. For this work, a 1/10th cosine function has been used:

$$
\begin{array}{ll}
h'(t) = h(t)\times(1 + \cos(\pi t/(0.1N - 1)))/2 & 0 \le t < 0.1N \\
h'(t) = h(t) & 0.1N \le t \le 0.9N \\
h'(t) = h(t)\times(1 + \cos(\pi(N-t)/(0.1N - 1)))/2 & 0.9N < t \le N
\end{array}
$$

where

$h(t)$ is the original time record,
$h'(t)$ is the new time record,
t is the sample number within the time record, and
N is the total number of samples in the time record.

While the MEM technique inherently produces smooth spectra, the FFT can be expected to give a spectrum with a lot of scatter (it can be shown that the discrete Fourier transform of a noise signal has a standard error for any given frequency equal to the power spectral density for that frequency). Consequently some form of smoothing may be applied to the spectrum in order to reduce the error. In this work two forms of smoothing have been used. For spectra obtained from individual time records the power spectral density at each point has been smoothed by means of a 7-point Golay–Savitsky convolution technique. In addition, since the evidence suggests that, with the exception of the time record in which failure occurred, the time records are essentially the same, an ensemble spectrum has been derived by taking the average of all of the individual spectra (before smoothing). It should be noted that smoothing of the spectrum in the frequency domain and windowing of the data in the time domain are closely related processes.

Whereas the discrete Fourier transform computes the coefficients of a series of sinewaves that sum to the observed time record, the maximum entropy method effectively computes the coefficients of a particular class of digital filter that would give the observed time record when applied to a white noise input signal. This has the advantages of making least assumptions about the behavior of the signal outside the sample period (this is the source of the name of the technique) and of producing smooth spectra. The method is particularly suitable for detecting sharp peaks in relatively short time records. However, some care must be used in the analysis, as rounding errors may cause problems with long time records, and the use of excessive numbers of coefficients can lead to the development of spurious peaks. The latter problem can usually be avoided by the use of a criterion due to Akaike[7] to determine the optimum number of coefficients, and this approach has been used in this work. All calculations have been performed using floating point arithmetic to the double-precision (64-bit) IEEE(3) standard, and rounding errors are thought to be insignificant.

---

(3) Institute of Electrical and Electronics Engineers (IEEE), New York, NY.

For various reasons, particularly because it tends to give straight lines for typical physical processes, the power spectrum is usually plotted in terms of log (power spectral density) vs log (frequency). While this is a perfectly acceptable method of presentation, it has led to a common error being promulgated in the corrosion literature. In order to express the limits on the validity of the spectral estimate which result from the discrete nature of the analyses, it is common practice to specify the range of validity as $-f_n$ to $+f_n$, where f_n is the Nyquist frequency. This has resulted in an assumption that the analysis can be extrapolated to very low frequencies. However, for a time record of total duration t, the bandwidth of the spectral estimate can be no less than 1/t. In other words one cannot tell anything about frequencies that correspond to a period longer than the time record. Trend-removal, windowing, and smoothing methods may further increase the bandwidth of the estimate, and as a result, one should be very careful about placing undue emphasis on the lower frequencies in the spectrum, just as aliasing and related problems should lead to caution in the interpretation of results close to the Nyquist frequency.

In addition to calculating the power spectral density as a function of frequency, the average power in the signal was also calculated as an overall measure of the activity of the system. This is often referred to in the corrosion literature as the standard deviation of the noise signal, and is generally found to be a measure of the rate of corrosion of the specimen. This parameter can be determined either by taking the time-based root-mean square of the potential (after trend removal), or by integrating the area under the power spectral density curve. The former technique has been used in this work.

Surface Replication

In order to follow the development of surface defects during a test, plastic replicas were taken at intervals during one test. These intervals corresponded to the end of individual time records, thus replicas were taken after every 20 minutes on test, although the cleaning and drying necessary for the replication meant that this period was considerably extended. It was found at the time records obtained for this test were much more variable than those for other experiments. Examination of the replicas revealed signs of general corrosion of the specimen surface (Figure 4 shows a replica taken after 1.5 hours on test), with no evidence of cracks prior to specimen failure.

RESULTS

Power Spectra

Typical curves of power spectral density vs frequency are shown in Figures 5 through 7. In general, it can be seen that the MEM and FFT analyses give very similar curves, although the MEM gives a much smoother curve. Attempts to improve the smoothness of the FFT by convolution did not give a very marked improvement in the visual appearance of the spectra, and other than Figure 8, all the FFT are presented in their "raw" form.

Both the MEM and (to a lesser extent) the FFT spectra tend to indicate a low-frequency plateau in the spectra. However, in view of the possible effects of trend removal, there must be some question as to how genuine this plateau is. If the mean of the time record is not removed, the MEM analysis shows no sign of a low frequency plateau, while the plateau becomes more pronounced as first the mean and then the linear trend are removed. Thus, without the benefit of an analysis made with a much longer time record, the low-frequency plateau must be regarded as a probable artifact of the analysis.

The more valid outcome of the analyses is the linear response in the intermediate frequency range, with a slope of the order −15 to −20 dB per decade. This implies a relationship of the form:

FIGURE 4. *SEM micrograph of specimen after exposure for 2 hours.*

$$V_n = V_o / f^b \tag{5}$$

where

V_n = voltage noise density at frequency f,
b = a constant, = 1, and
V_o = voltage noise density at 1 Hz.

The final fracture of the specimen appears to give a single large potential transient, with an amplitude of the order of 40 mV. This transient gives rise to a much higher power spectral density at any given frequency, and there is also a tendency for the slope in the intermediate frequency region to be shallower (around 12 to 15 dB per decade), but the significance of this difference is somewhat questionable.

Some spectra (e.g., Figure 6[c]) show evidence of peaks in the high-frequency range (0.1 to 1 Hz). While this is clearly a real effect, in that it is not an artifact of the data collection or analysis procedures, its significance remains uncertain.

At the higher frequency end of the spectra there is a tendency for the curve to flatten out, as if approaching a second plateau. However, this is probably explained by the absence of anti-aliasing filters in the measuring system. Figure 9 shows the calculated effect of the "folding back" of the frequencies above the Nyquist frequency for a pure 1/f response, and it can be seen that this has a very similar appearance to the spectra actually obtained. Without further data collection at higher frequencies it seems reasonable to assume that the 1/f response continues to frequencies above 1 Hz.

RM Noise Voltage

Figure 10(b) shows the variation in the RMS voltage (which is equivalent to both the square root of the average noise power and the standard deviation of the time record after trend removal) for the first 9 time records for one test, in which the specimen was stressed and failed in time record 8, and a second test in which the specimen was not stressed. It can be seen that, with only two exceptions, both specimens show a low and reasonably constant noise voltage over all records. The first exception is due to a short-lived initial transient for the unstressed specimen, and is not thought to be significant. The other exception is the large increase observed at approximately 160 minutes for the stressed specimen, which corresponded to failure of the specimen. This can also be seen in Figure 10(a), where the time records for the two specimens are plotted. Owing to the highly compressed scale (each of the composite time records contains over 9000 points), the fine detail of the time records cannot be resolved, but the width of the local fluctuations (which correlates approximately with the average

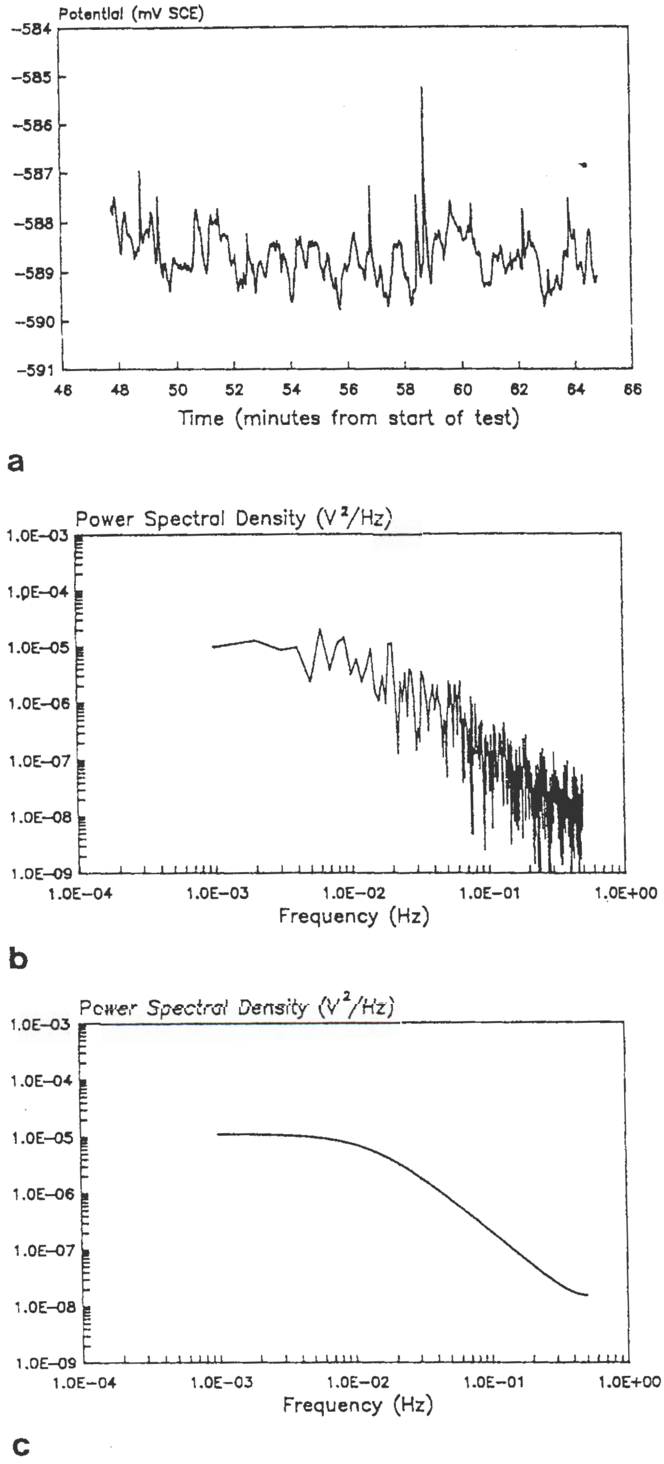

FIGURE 5. *Power spectral density for an unstressed specimen for the period from 40 to 57 minutes after immersion: (a) time record, (b) FFT spectrum, (c) MEM spectrum.*

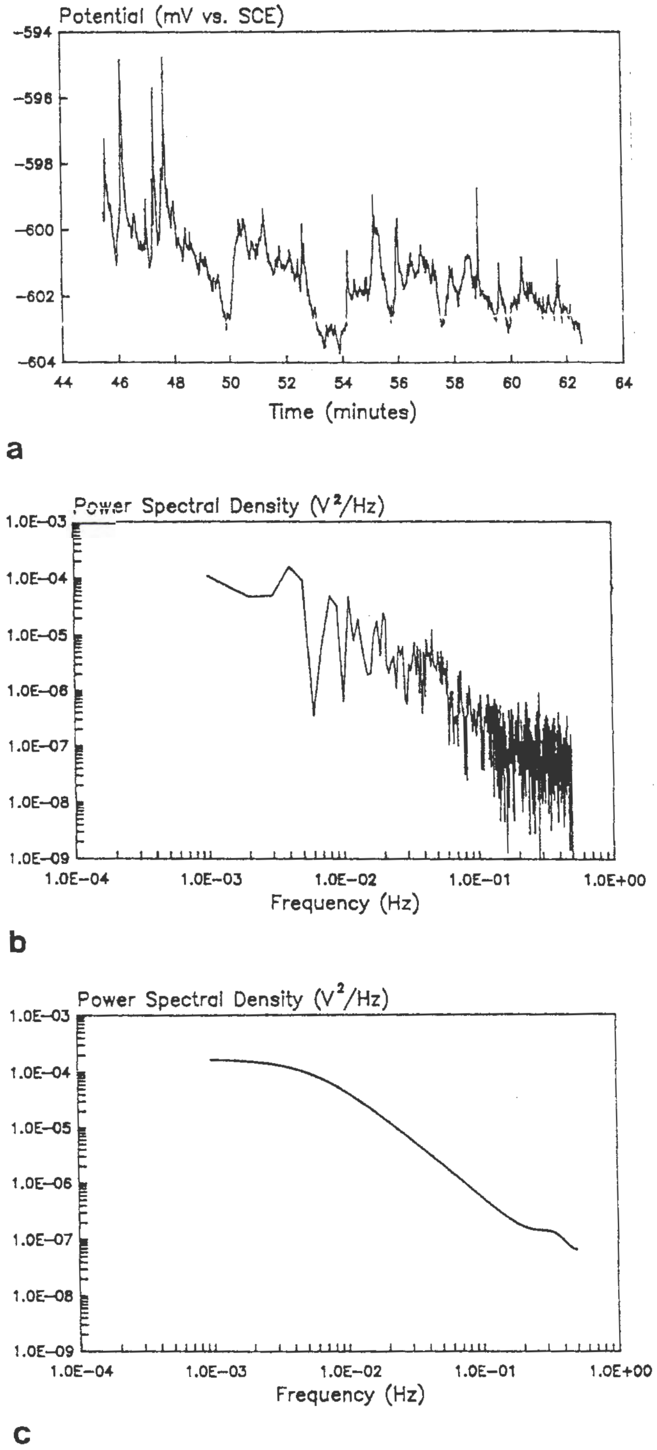

FIGURE 6. *Power spectral density for a stressed specimen for the period from 40 to 57 minutes after immersion: (a) time record, (b) FFT spectrum, (c) MEM spectrum.*

noise voltage), and the large single peak in time record 8 are clearly visible.

Further Analysis

In the case of the stressed specimen for which data are presented in Figure 10, there was no evidence of transient events prior to final fracture. However, in another experiment there was evidence of small transients occurring before final fracture. This is shown in terms of the sequence of time records, together with the associated noise voltage, in Figures 11(a) and 11(b). It is not possible to say whether these transients were also associated with a crack advance event, but this does seem probable. It is clear from Figure 11 that the power spectra and noise voltage are rather poor predictors of the presence of transient events. Further consideration of the nature of individual transients suggests that, at least in part, this is because the length of time record used in this work (1024 seconds) is significantly greater than the duration of a typical transient event (about 60 seconds). In order to determine whether the existing analytical techniques could provide a better

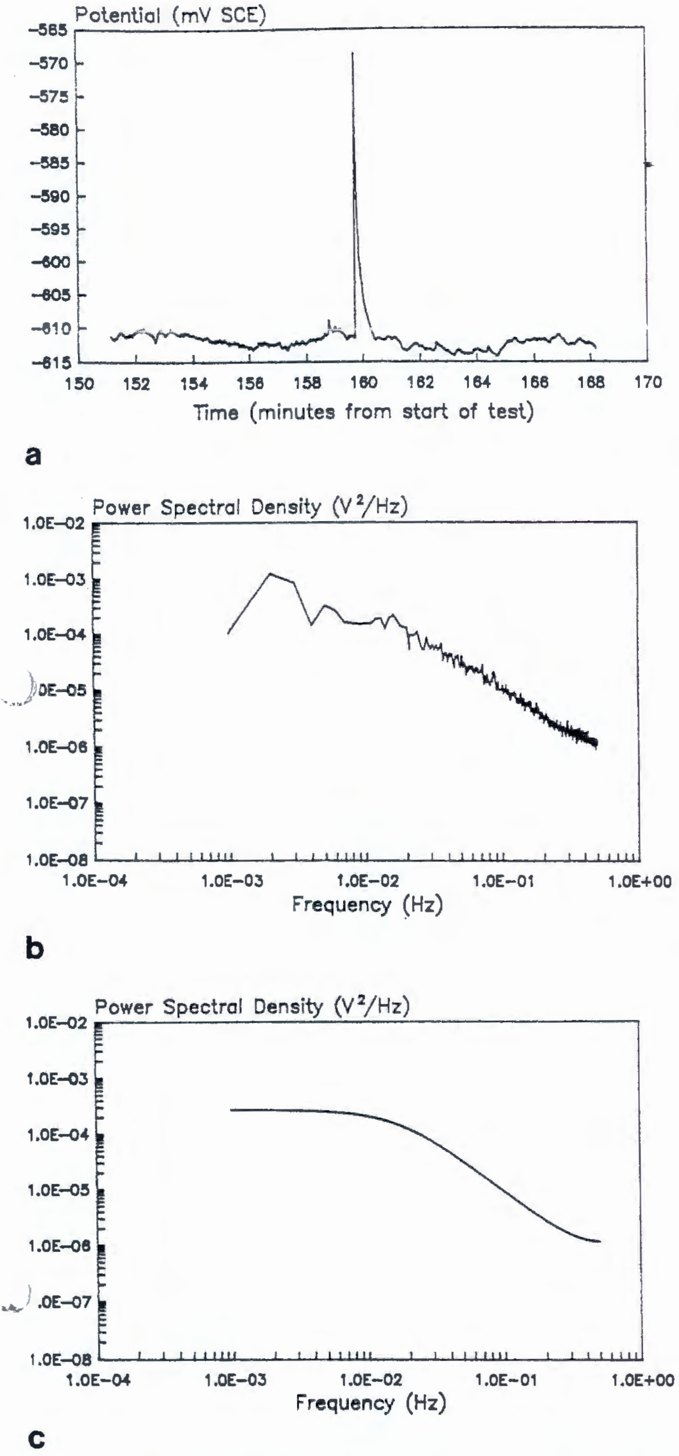

FIGURE 7. *Power spectral density for a stressed specimen for the period from 140 to 1 57 minutes after immersion: (a) Time record, (b) FFT spectrum, (c) MEM spectrum. This specimen fractured during the measurement of this time record.*

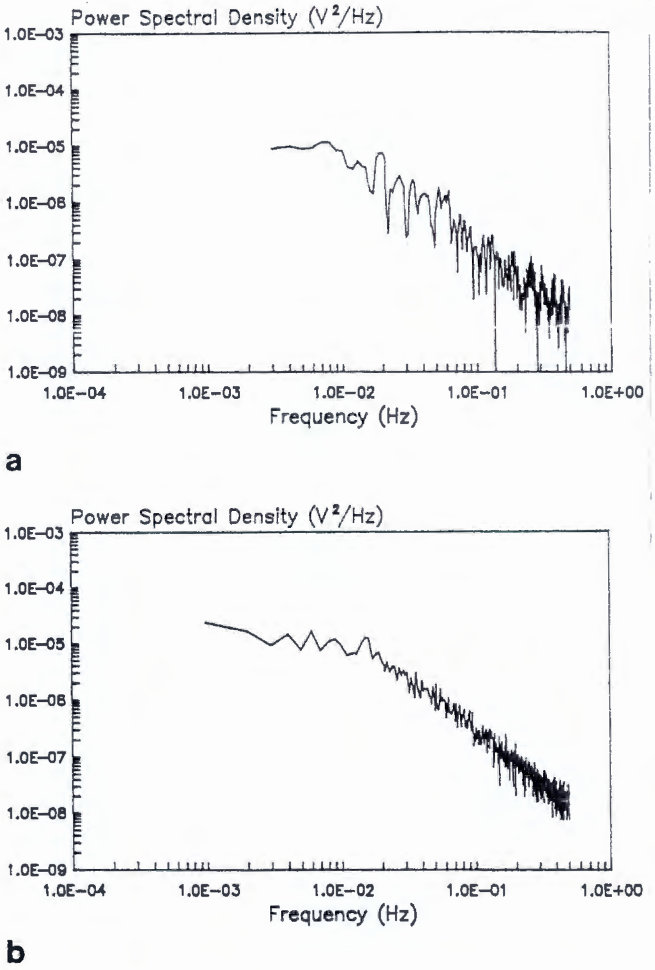

FIGURE 8. *Power spectral density for the experiment of Figure 5, computed by FFT with smoothing: (a) Savitsky–Golay smoothing of time record 3 (as Figure 5[b]) (b) Ensemble spectrum for 9 the records.*

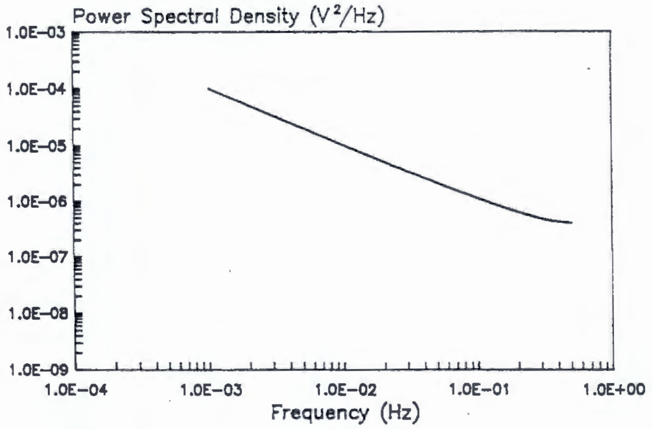

FIGURE 9. *Computed effect of aliasing on a pure 1/f response.*

indication of the occurrence of a transient associated with cracking, the time records of Figure 11(a) have been re-analyzed using a record length of 64. Thus each 1024 point time record gives rise to 16 spectra and values of noise voltage, each corresponding to a 64 second time record. The results of this analysis are summarized in Figure 11(c), in which the noise voltage is plotted as a function of time from the beginning of the test. In this figure the peaks in noise voltage associated with the transients occurring after 33 and 79 minutes show up very clearly, with some indication of smaller transients at about 46, 65, and 70 minutes. The corresponding spectra necessarily show a higher level of noise at these peaks, but there is little indication of any other difference. Thus it is suggested that the average noise power, measured over a time comparable to the duration of a typical transient, is an effective method for the detection of transients associated with crack propagation. Visual examination of the time record is also very effective

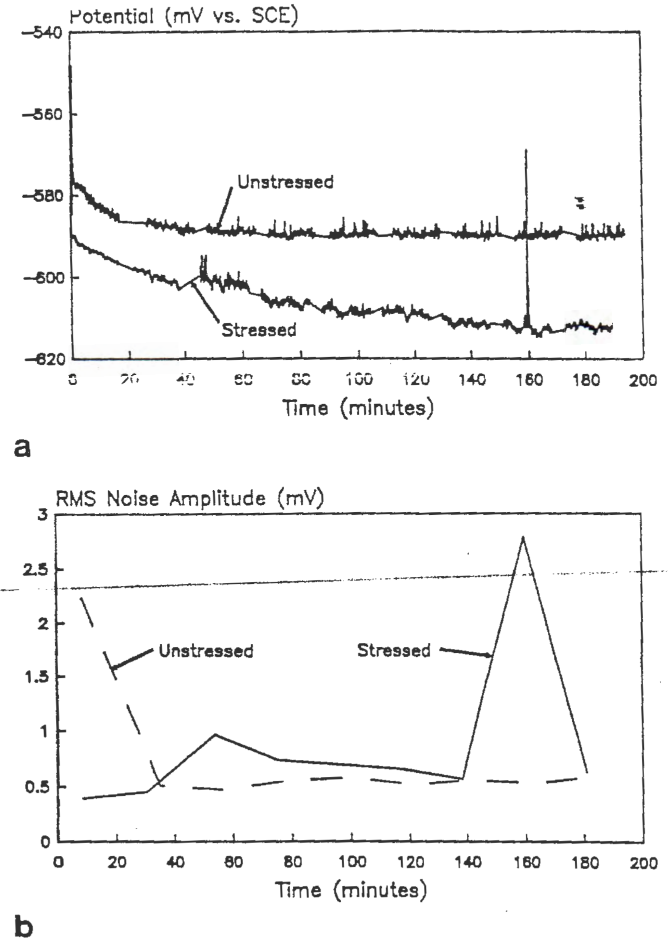

FIGURE 10. *Time records and noise voltage for stressed and unstressed specimens: (a) first 9 time records, (b) RM noise voltage (averaged over full time records) for first 9 time records.*

for detecting transients, and this might be further assisted by the addition of a high pass filter to eliminate the slower fluctuations in potential. For serious application as a monitoring technique for hydrogen embrittlement crack growth, it seems probable that it would be necessary to detect much smaller transients than those which we have observed, and currently it seems unlikely that his will be feasible in realistic conditions, without further development of techniques for the extraction of transients from the time record.

Mechanistic Implications

One of the reasons for the selection of this environmental cracking system for study was the certainty with which the crack growth process could be attributed to hydrogen embrittlement. This is commonly supposed to proceed discontinuously, with hydrogen generated at the metal surface diffusing into the steel and initiating brittle fracture. The fact that the noise spectra for stressed and unstressed specimens are essentially identical, with the exception of intermittent transients (which are presumed to be associated with crack advance), is consistent with this model of crack growth.

CONCLUSIONS

▶ Electrochemical noise monitoring shows a distinct transient in the electrochemical potential associated with failure by hydrogen embrittlement of a high-strength steel.

▶ There is some evidence of smaller transients occurring prior to final fracture. These are probably associated with crack advance, although this has not been proved.

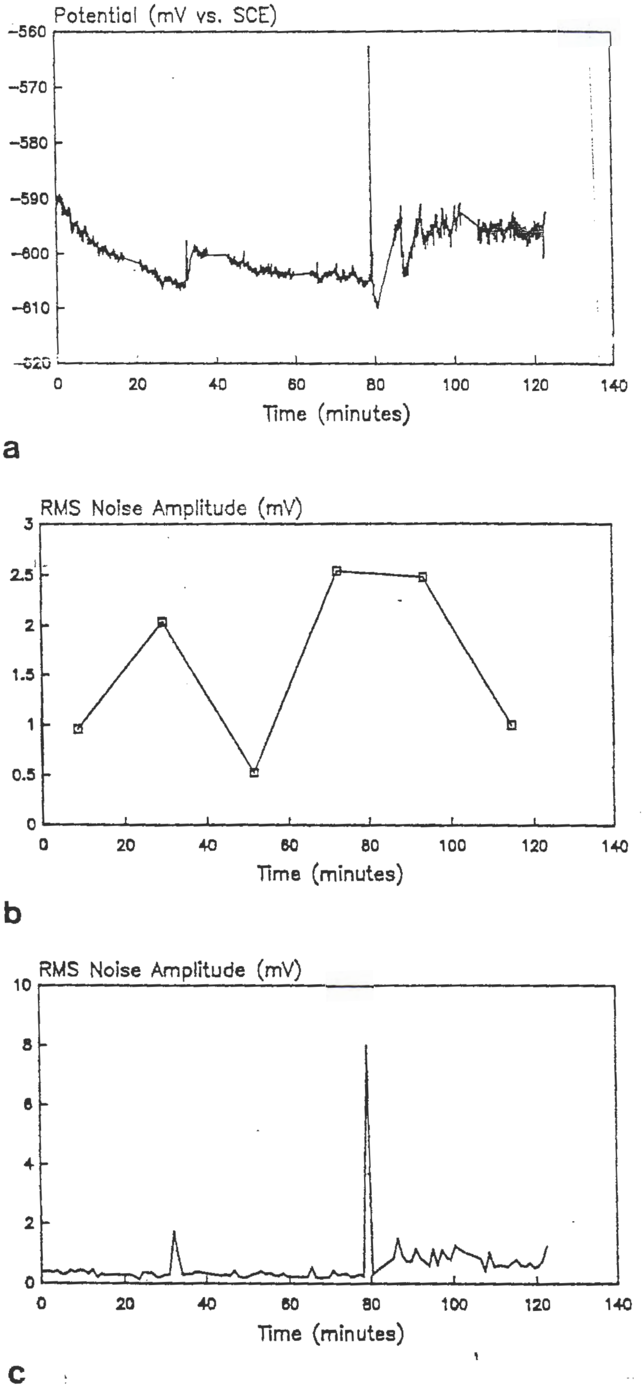

FIGURE 11. *Time records and noise voltage for a specimen showing transients prior to final fracture: (a) time records, (b) RM noise voltage (averaged over full time records), (c) RMS noise voltage (averaged over groups of 64 samples).*

▶ The power spectra obtained show a significant increase in amplitude when a failure transient occurs, but the general form of the spectra remains essentially unchanged.

▶ The only component of the spectra that can be specified with any certainty is the roll-off in the intermediate frequency range, which has approximate 1/f characteristics.

- ▶ Features observed at low frequencies (0.001 to 0.01 Hz) are strongly dependent on analysis procedures and are regarded as unreliable.

- ▶ At high frequencies (0.1 to 1 Hz), there is occasional evidence of structure in the spectra, although the significance of this remains uncertain. There is also a minor artifact in these data that results from aliasing.

ACKNOWLEDGMENTS

This work was performed by one of the authors (CAL) with the support of the Federal Government of Nigeria. The data acquisition and initial analysis employed programs written by Dr K. Hladky. The authors thank the head of the Corrosion and Protection Centre for the provision of laboratory facilities.

REFERENCES

1. G. Blanc, C. Gabrielli, and M. Keddam, Electrochimica Acta 20(1975): p. 687-689.
2. K. Hladky and J.L. Dawson, Corrosion Science, 21(1981): p. 317.
3. W.P. Iverson, J. Electrochem. Soc. 115(1968): p. 617-618.
4. U. Bertocci and J. Kruger, Surf. Sci. 101(1980): p. 608-618.
5. U. Bertocci, J. Electrochem. Soc. 127(1980): p. 1931-1934.
6. J.P. Burg, in Modern Spectrum Analysis, ed. D.G. Childers (New York, NY: IEEE, 1978), p. 42-48.
7. H. Akaike, Annals Inst. Statis. Math. 21(1969): p. 243-247.

Discussion on *"Technical Note:* Potential–pH Diagrams for the Fe–Cl^-–H_2O System at 25 to 150°C" ☆

INTRODUCTION

The following article discusses *"Technical Note:* Potential–pH Diagrams for the Fe–Cl^-–H_2O System at 25 to 150°C," by S. Kesavan, T.A. Mozhi, B.E. Wilde, which was published in *Corrosion* 45, 3(1989): p. 213. A reply from Kesavan follows.

DISCUSSION(1)

The following discussion is by P. Paine (EPRI).(2)

I have a few comments concerning the Technical Note in the March 1989 issue, on page 213 by Kesavan et al. The authors would predict that steam generators are filled with hematite (Fe_2O_3), rather than magnetite (Fe_3O_4), at operating temperatures above 150°C.

Steam generators operate at about the hydrogen evolution potential at bulk water pHs of 5.5 to 6.0 (at 280°C, 553°K). The oxygen concentration, while very low, is not negligible in a lot of cases. We do not normally operate with saturated NaCl, but in going from Fe to Fe_3O_4 to Fe_2O_3, chloride ion concentration should not enter into the equation.

In trying to see what is "wrong" with the potential–pH diagrams, I observe that their thermodynamic data comes from the 1952 NBS(3) values rather than from more recent JANAF(4) or other publications.

I had Dr. D.D. Cubicciotti, a member of our staff, calculate the Fe system from newer data. I have attached plots at 473 (Figure D1) and 573°K (Figure D2), but at 10^{-6} rather than saturated NaCl. This data correctly predicts the actual operating experience, i.e., magnetite.

---

(1) Submitted for publication May 1989.

(2) EPRI, 3412 Hillview, P.O. Box 10412, Palo Alto, CA 94303.

(3) Formerly the National Bureau of Standards (NBS), now the National Institute of Standards and Technology (NIST), Washington, DC.

(4) D.R. Stull and H. Prophet, JANAF Thermochemical Tables, 2nd ed., NSRDS-NBS 37 (Washington, DC: U.S. Govt. Printing Office, 1971).

REPLY(1)

The following reply is by S. Kesavan and B.E. Wilde (Ohio State University).(2)

We thank Dr. Paine for his observation. After checking our calculations again, we found that an error was made not in our calculations but in plotting the hydrogen evolution (a) and oxygen reduction (b) lines on our Pourbaix diagrams. A corrected version of the diagrams (Figures R1 through R4) has been plotted. From these diagrams, it is clearly evident that Fe_3O_4 is the stable species for the practical conditions cited by Dr. Paine. Our results agree with those of Paine et. al. We do not think that thermodynamic data from the 1952 NBS publication has introduced significant error in our results.

---

(1) Submitted for publication October 1989.

(2) Fontana Corrosion Center, Dept. of Metallurgical Engineering, Ohio State University, 116 West 19th Ave., Columbus, OH 43210.

0010-9312/90/000005/$3.00/0